

Generalized Phase Shifting for M -Band Discrete Wavelet Packet Transforms

Yiannis Andreopoulos and Mihaela van der Schaar

Abstract—This correspondence presents a novel method for the construction of translation-invariant discrete wavelet packet (TIDWP) transforms for any decomposition level k , starting from any phase of a critically sampled discrete wavelet-packet representation of level k . The process is performed by phase shifting, i.e., the direct recovering of the wavelet coefficients omitted by the downsampling operations of each decomposition level without reconstructing the input signal. The proposed method enables tradeoffs between memory utilization and computational efficiency for the construction of translation-invariant representations. Hence, it is useful in resource-constrained TIDWP-based applications of digital signal compression, image segmentation and detection of transients.

Index Terms—Best-basis selection, complexity and memory aspects, overcomplete discrete wavelet packet (WP) transforms, translation invariance.

I. INTRODUCTION

Wavelet packet (WP) transforms represent a generalization of the method of multiresolution decomposition and comprise the entire family of subband (tree) decompositions [1]. They offer fast access to a rich menu of bases from which the “best basis” can be chosen [2], [3]. The basic framework was extended to include translation-invariant representations by numerous researchers [4]–[8] in order to treat signals with transient or nonlinear behavior. The importance of (near) translation-invariant representations is highlighted also by recent research advances in the context of Hilbert and tight frame wavelets [9], [10]. Translation-invariant discrete wavelet packet (TIDWP) transforms have already been used in a variety of contexts like transient signal detection [6], feature extraction for texture and image segmentation [11], [12], image [4], audio [13] and signal compression [14], [15] and location establishment of complicated events from discrete measurements [16]. For the vast majority of these applications, the TIDWP decomposition is performed up to a certain decomposition level; then a best-basis selection algorithm is applied using an appropriate cost function, such as the entropy or threshold-counting metrics [2], [4], or textural measures [11]. Best-basis algorithms begin from the TIDWP decomposition of a certain level k [4], [14] and operate in a bottom-up manner (coarse-to-fine resolution) to identify the subbands that contain the most significant features for the application of interest, with respect to the given cost function. In this way, the complexity of the decomposition and best-basis selection is guaranteed to be $O(N \log_M N)$ for an N -sample signal analyzed by an M -band system [2], [14].

Manuscript received July 18, 2005; revised February 12, 2006. The associate editor coordinating the review of this manuscript and approving it for publication was Dr. Ta-Hsin Li. The authors would like to acknowledge the kind support of the National Science Foundation: NSF CCF-0541867 (CAREER Award), NSF CCF-0541453 and NSF-CNS-0509522, as well as the support from UC Micro.

Y. Andreopoulos was with the Department of Electrical Engineering (EE), University of California Los Angeles (UCLA), Los Angeles, CA 90095-1594 USA. He is now with the Department of Electronic Engineering, Queen Mary University of London, E1 4NS London, U.K. (e-mail: yiannis.a@elec.qmul.ac.uk).

M. van der Schaar is with the Department of Electrical Engineering (EE), University of California, Los Angeles (UCLA), Los Angeles, CA 90095-1594 USA (e-mail: mihaela@ee.ucla.edu).

Digital Object Identifier 10.1109/TSP.2006.885743

The good performance of TIDWP transforms stems from the fact that good frequency localization is provided and, unlike the conventional WP transforms, the temporal resolution is not sacrificed since the effect of downsampling is alleviated by periodic translation of the input [4]. Fig. 1 presents a pictorial explanation for a two-band system. For each decomposition level k , all the low-pass and bandpass subbands¹ ($A_m^{k-1}(z)$ and $D_m^{k-1}(z)$ respectively, with $0 \leq m \leq 2^{k-1} - 1$ indicating the wavelet-packet number), or the input signal $X(z)$ for $k = 1$, are decomposed by the critically-sampled discrete wavelet transform. For any level $k = 1, 2, 3$ in Fig. 1, if we define a discrete wavelet packet as $[\mathbf{w}_m^k(z)]_0 = [A_m^k(z)]_0 [D_m^k(z)]_0^T$, the critically sampled (complete) WP transform consists of packets $[\mathbf{w}_0^1(z)]_0$ for $k = 1$, $[\mathbf{w}_0^2(z)]_0$ and $[\mathbf{w}_1^2(z)]_0$ for $k = 2$, and finally $[\mathbf{w}_0^3(z)]_0$, $[\mathbf{w}_1^3(z)]_0$, $[\mathbf{w}_2^3(z)]_0$ and $[\mathbf{w}_3^3(z)]_0$ for $k = 3$ [6]. However, in order to provide translation invariance, one must also obtain the alternate polyphase components for each decomposition of each level k [17]–[20]. This leads to the all-phase [18], [19] discrete wavelet packet decomposition, i.e., the TIDWP transform [4]–[6], which is overcomplete with a redundancy of M^k for an M -band decomposition at level k .

In Section II, based on prior work [17]–[20], we present a method for the construction of any phase component n_d of the M -band TIDWP of level k , starting from a complete WP decomposition of level k that may be of arbitrary phase n_s , with $0 \leq n_s, n_d \leq M^k - 1$ and $n_s \neq n_d$. The benefits of the proposed approach are in the flexibility offered for trading off memory for computational resources in TIDWP transform applications (e.g., best-basis selection algorithms), as explained in Section III. Experimental results are presented in order to instantiate the benefit of such tradeoffs in a real system. Our conclusions are presented in Section IV.

II. PHASE SHIFTING IN TIDWP TRANSFORMS

A. General

Starting from the basic multirate identities [21], in the general case of subsampling by M , the polyphase separation of a signal $X(z)$ is given by $\mathcal{D}X(z) = [[X(z)]_0 \dots [X(z)]_{M-1}]^T$, with the commutative operation given by $\mathcal{D}^{-1}\mathcal{D}X(z) = \sum_{m=0}^{M-1} z^m [X(z^M)]_m = X(z)$. The Type-I analysis polyphase matrix that produces the zeroth polyphase component of the M -band discrete wavelet transform is denoted by $\mathbf{E}_0(z)$; its definition is

$$\mathbf{E}_0(z) = \begin{bmatrix} [H_0(z)]_0 & \dots & [H_0(z)]_{M-1} \\ \vdots & \ddots & \vdots \\ [H_{M-1}(z)]_0 & \dots & [H_{M-1}(z)]_{M-1} \end{bmatrix} \quad (1)$$

with $H_m(z)$ the m th analysis filter ($0 \leq m \leq M - 1$). Correspondingly, for the m th polyphase component of the transform decomposition, $1 \leq m \leq M - 1$, we have

$$\mathbf{E}_m(z) = \mathbf{E}_0(z)\mathbf{P}_m(z) \quad (2)$$

with

$$\mathbf{P}_m(z) = z \begin{bmatrix} \mathbf{0} & \mathbf{I}_m \\ z^{-1}\mathbf{I}_{M-m} & \mathbf{0} \end{bmatrix}$$

¹All signals and filters are considered in the Z -domain as Laurent polynomials, and the letter z is reserved for this purpose. All the used indexes are integers. For all matrices, vectors, signals and filters, the superscripts denote the decomposition level, except for superscript T that denotes transposition. Subscripts are used to enumerate signals or filters in matrices and vectors. In addition, notation $[Q(z)]_i$ indicates the Type-I i th polyphase component of signal or filter $Q(z)$ [20], $(x)_M$ denotes the base- M representation of scalar x ($M > 1$), and $\lfloor x \rfloor$ denotes the largest integer not greater than x .

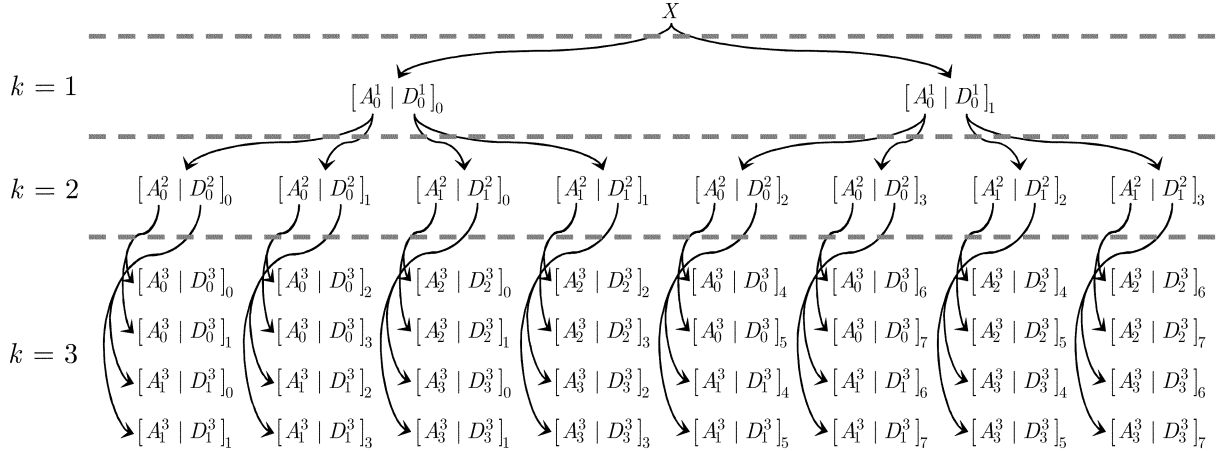


Fig. 1. Two-band translation invariant discrete wavelet packet decomposition of signal $X(z)$ for decomposition levels $k = \{1, 2, 3\}$.

denoting the pseudocirculant matrix² [21]. For example, based on (1), for the case of $M = 2$ corresponding to Fig. 1, we have $[A_0^1(z)]_m = [D(z^m H_0(z))]^T D X(z)$ and $[D_0^1(z)]_m = [D(z^m H_1(z))]^T D X(z)$. The corresponding Type-II synthesis polyphase matrices are $\mathbf{R}_m(z) = [\mathbf{E}_m(z)]^{-1}$, i.e.,

$$\mathbf{R}_0(z) = (\mathbf{E}_0(z))^{-1} \quad (3)$$

for $m = 0$, and for any $1 \leq m \leq M - 1$, we have

$$\mathbf{R}_m(z) = z^{-1} \mathbf{P}_{M-m}(z) \mathbf{R}_0(z) \quad (4)$$

based on the properties of the pseudocirculant matrix [21]. In order to simplify the expressions, we always assume (without loss of generality) that $\det \mathbf{E}_0(z) = a$, $a \neq 0$.

B. Generalized Phase Shifting for $M \geq 2$

For the generic case of an M -band TIDWP transform, for any decomposition level k , we shall study the construction of any WP m of phase n_d (destination phase component) from the WPs of phase n_s (starting phase component), where $0 \leq n_s, n_d \leq M^k - 1$ and $0 \leq m \leq M^{k-1} - 1$. Moreover, since M bandpass filters are applied at every decomposition level, M subbands are contained in each WP m , denoted by $[\mathbf{w}_m^k(z)]_{n_s} = [[S_{0,m}^k(z)]_{n_s} \ \dots \ [S_{M-1,m}^k(z)]_{n_s}]^T$ (for phase n_s of level k). For the example of Fig. 1, we have $[S_{0,m}^k(z)]_{n_s} = [A_m^k(z)]_{n_s}$ and $[S_{1,m}^k(z)]_{n_s} = [D_m^k(z)]_{n_s}$. The following two propositions present the case of decomposition levels one and two, respectively, and facilitate the understanding of the general proposition for an arbitrary level $E = k$.

Proposition 1—Generalization of Proposition 1 in [19] and of the Basic solution in [18] and of Prediction Rule 1 of [17]: For an M -band perfect reconstruction filter bank with $E = 1$ decomposition level, the construction of the WP of phase n_d by the WP of phase n_s , with $0 \leq n_s, n_d \leq M - 1$, and $n_s \neq n_d$ is performed as

$$[\mathbf{w}_0^1(z)]_{n_d} = \mathbf{F}^1(z) [\mathbf{w}_0^1(z)]_{n_s} \quad (5)$$

²The pseudocirculant matrix is multiplied by z since, similar to our prior work [18], [19], we are shifting the analysis filters instead of the input signal. Both approaches are equivalent, but shifting the analysis filters facilitates the actual implementation.

with the phase-shifting matrix of level one given by

$$\mathbf{F}^1(z) = \begin{bmatrix} F_{0,0}^1(z) & \dots & F_{0,M-1}^1(z) \\ \vdots & \ddots & \vdots \\ F_{M-1,0}^1(z) & \dots & F_{M-1,M-1}^1(z) \end{bmatrix} = z^{-1+[\lceil r/M \rceil]} \mathbf{E}_{r \bmod M}(z) \mathbf{R}_0(z) \quad (6)$$

where $r = M + n_d - n_s$, $a \bmod b = a - b[a/b]$ the modulo operation ($a, b \in \mathbb{N}_+$), and $F_{i,j}^1(z)$ are the phase-shifting filters of level one, $0 \leq i, j \leq M - 1$.

Proof: We can reach (5) by performing an inverse transform to subbands $[\mathbf{w}_0^1(z)]_{n_s}$ followed by a forward wavelet transform that retains the n_d polyphase components of the nondecimated decomposition [18], [19], i.e.,

$$[\mathbf{w}_0^1(z)]_{n_d} = \mathbf{E}_{n_d}(z) \mathbf{D} \mathbf{D}^{-1} \mathbf{R}_{n_s}(z) [\mathbf{w}_0^1(z)]_{n_s}. \quad (7)$$

An example can be seen in Fig. 1 for $M = 2$. In order to obtain the final result, we replace the analysis and synthesis polyphase matrices based on (2) and (4), and the following property is used for the product of two pseudocirculant matrices [21], for any $0 \leq n_s, n_d \leq M - 1$, as follows:

$$\text{if } n_s + n_d \neq M : \mathbf{P}_{n_s}(z) \mathbf{P}_{n_d}(z) = z^{\lfloor (n_s + n_d)/M \rfloor} \times \mathbf{P}_{(n_s + n_d) \bmod M}(z) \quad (8)$$

$$\text{if } n_s + n_d = M : \mathbf{P}_{n_s}(z) \mathbf{P}_{n_d}(z) = z \cdot \mathbf{I}. \quad (9)$$

Numerical examples of the derived filters from Proposition 1 for popular filter banks with $M = 2$, $n_s = 0$, $n_d = 1$ can be found in our recent work [20].

Proposition 2: For an M -band perfect reconstruction filter bank with $E = 2$, the construction of WPs $[\mathbf{w}_m^2(z)]_{n_d}$, $0 \leq m \leq M - 1$, by the M WPs $[\mathbf{w}_0^2(z)]_{n_s}, \dots, [\mathbf{w}_{M-1}^2(z)]_{n_s}$, with $0 \leq n_s, n_d \leq M^2 - 1$ and $n_s \neq n_d$ is performed as

$$[\mathbf{w}_m^2(z)]_{n_d} = \sum_{i=0}^{M^l-1} \mathbf{F}_{m,i}^{l+1}(z) [\mathbf{w}_{M^l \lfloor m/M^l \rfloor + i}^2(z)]_{n_s} \quad (10)$$

where $l = \lceil \log_M((n_d)_M \oplus (n_s)_M) \rceil$ with $(a)_M \oplus (b)_M$ the base- M XOR operation³ between scalars a and b ($a, b \in \mathbb{N}$), and we set

³For $M > 2$, i.e., for a ternary, quaternary base, etc., the XOR function is considered as carry-free addition, i.e., the addition operation per digit of base M , modulo M .

TABLE I

PHASE-SHIFTING FILTERS FOR THE 9/7 FILTER BANK ($M = 2$, $\det \mathbf{E}_0(z) = -1$) FOR THE CASE OF $k = 2$, $l = 1$, $m = 0$, $n_s = 1$, AND $n_d = 2$. THE FILTER TAPS ARE REPORTED STARTING FROM THE MAXIMUM ORDER IN z (WHICH IS z^6 IN THIS CASE)

$G_{0,0}^2(z)$	$G_{0,1}^2(z)$	$G_{1,0}^2(z)$	$G_{1,1}^2(z)$	$G_{0,2}^2(z)$	$G_{0,3}^2(z)$	$G_{1,2}^2(z)$	$G_{1,3}^2(z)$
0.00000596	-0.00000349	0.00001017	-0.00000596				
0.00023365	-0.00014937	0.00036249	-0.00023365	0.00001017	-0.00000596	0.00001735	-0.00001017
-0.00403046	0.00169389	-0.00869377	0.00403047	0.00035200	-0.00022750	0.00053890	-0.00035200
0.02710342	-0.01586242	0.05464973	-0.02710342	-0.00347634	0.00099419	-0.00874897	0.00347634
-0.12007284	0.09377374	-0.14082618	0.16792440	0.01522389	-0.01454260	0.02284002	-0.01522389
0.88179588	-0.24526494	0.17732658	-0.31449318	-0.03549481	0.04002711	-0.01464730	0.14673890
0.26671171	0.31072164	-0.11091074	-0.50596952	0.04677016	-0.02624524	-0.01464730	0.48740582
-0.06254196	-0.19238483	0.02934202	0.05765915	-0.03549481	-0.02624524	0.02284002	0.14673890
0.01174092	0.05005002	-0.00116063	-0.01174092	0.01522389	0.04002711	-0.00874897	-0.01522389
-0.00088787	-0.00325057	-0.00009966	0.00088787	-0.00347634	-0.01454260	0.00053890	0.00347634
-0.00005841	0.00064208		0.00005841	0.00035200	0.00099419	0.00001735	-0.00035200
	0.00003424			0.00001017	-0.00022750		-0.00001017
					-0.00000596		

$\forall m, i : \mathbf{F}_{m,i}^1(z) \equiv \mathbf{F}^1(z)$. Moreover, the phase-shifting matrices of level two, $\mathbf{F}_{m,i}^2(z)$, are defined as

$$\mathbf{F}_{m,i}^2(z) = \mathbf{E}_{n_d \bmod M}(z) \cdot \left(\left[\mathbf{F}_{m,i}^1(z) \right]_0 \mathbf{I} + \sum_{q=1}^{M-1} z^{-1} \left[\mathbf{F}_{m,i}^1(z) \right]_q \mathbf{P}_q(z) \right) \cdot \mathbf{R}_{n_s \bmod M}(z) \quad (11)$$

where the filters $\mathbf{F}_{(m)(i)}^1(z)$ are defined by (6) with:

$$r = M + \left\lfloor \frac{n_d}{M} \right\rfloor - \left\lfloor \frac{n_s}{M} \right\rfloor. \quad (12)$$

Proof: See Appendix I.

The derived phase-shifting filters for the case of $k = 2$, $M = 2$, $m = 0$, $l = 0$, and $n_d > n_s$ correspond to the filters for $k = 1$, $M = 2$, $n_s = 0$, $n_d = 1$ [20]. For the case of $k = 2$, $M = 2$, $m = 0$, $l = 1$, if we select $n_d > n_s$, an example of the derived phase-shifting filters can be found in Table I. These filters suffice for the construction of the zero-numbered WPs of the TIDWP of $k = 2$ if successive phase shifting is used from phase $n_d - 1$ to n_d , $1 \leq n_d \leq 7$.

Proposition 2 indicates that, for decomposition levels beyond one, there is a number of phase-shifting matrices, each with their own filters. For notational simplicity, we can organize the phase shifting matrices of any level k into a global phase-shifting matrix based on the following definition.

Definition 1: For every decomposition level k , the global phase-shifting matrix is defined as

$$\mathbf{G}^k(z) = \begin{bmatrix} G_{0,0}^k(z) & \cdots & G_{0,M^k-1}^k(z) \\ \vdots & \ddots & \vdots \\ G_{M^k-1,0}^k(z) & \cdots & G_{M^k-1,M^k-1}^k(z) \\ \mathbf{F}_{0,0}^k(z) & \cdots & \mathbf{F}_{0,M^k-1}^k(z) \\ \vdots & \ddots & \vdots \\ \mathbf{F}_{M^k-1,0}^k(z) & \cdots & \mathbf{F}_{M^k-1,M^k-1}^k(z) \end{bmatrix}. \quad (13)$$

Definition 1 demonstrates that filter $G_{i,j}^k(z)$ in the global phase-shifting matrix of level k (with $0 \leq i, j < M^k$) is the phase-shifting filter at row $(i \bmod M)$ and column $(j \bmod M)$ of phase-shifting matrix $\mathbf{F}_{\lfloor i/M \rfloor, \lfloor j/M \rfloor}^k(z)$.

We now have enough insight to attempt a generalization of the WP phase construction for an arbitrary decomposition level k . Our result is given by the following proposition.

Proposition 3—Generalization of Proposition 2 for Any Level $E = k$: For an M -band perfect reconstruction filter bank with $E = k$, the

construction of any WP $[\mathbf{w}_m^k(z)]_{n_d}$, $0 \leq m \leq M^{k-1} - 1$, by the WPs $[\mathbf{w}_0^k(z)]_{n_s}, \dots, [\mathbf{w}_{M^{k-1}-1}^k(z)]_{n_s}$, with $0 \leq n_s, n_d \leq M^k - 1$, and $n_s \neq n_d$, is given by

$$[\mathbf{w}_m^k(z)]_{n_d} = \sum_{i=0}^{M^l-1} \mathbf{F}_{m,i}^{l+1}(z) [\mathbf{w}_{M^l \lfloor m/M^l \rfloor + i}^k(z)]_{n_s} \quad (14)$$

where $l = \lceil \log_M((n_d)_M \oplus (n_s)_M) \rceil$, and, we set $\forall m, i : \mathbf{F}_{m,i}^1(z) \equiv \mathbf{F}^1(z)$ for $l = 0$. For $l > 0$, the phase-shifting matrices $\mathbf{F}_{m,i}^{l+1}(z)$, are defined as

$$\mathbf{F}_{m,i}^{l+1}(z) = \mathbf{E}_{n_d \bmod M}(z) \cdot \left(\left[\mathbf{G}_{m,i}^l(z) \right]_0 \mathbf{I} + \sum_{q=1}^{M-1} z^{-1} \left[\mathbf{G}_{m,i}^l(z) \right]_q \mathbf{P}_q(z) \right) \cdot \mathbf{R}_{n_s \bmod M}(z) \quad (15)$$

where filters $G_{m,i}^l(z)$ correspond to matrix $\mathbf{F}^l(z)$ and hence are defined by (6) with

$$r = M + \left\lfloor \frac{n_d}{M} \right\rfloor - \left\lfloor \frac{n_s}{M} \right\rfloor \quad (16)$$

and filters $G_{m,i}^h(z)$, $2 \leq h \leq l$ are defined recursively by (15) with the following replacements:

$$l \leftarrow h - 1, \quad n_d \leftarrow \left\lfloor \frac{n_d}{M^{l+1-h}} \right\rfloor, \quad n_s \leftarrow \left\lfloor \frac{n_s}{M^{l+1-h}} \right\rfloor.$$

Proof: See Appendix II.

The last proposition demonstrates that the construction of an arbitrary WP of level k can be performed based on a subset, or the full set, of WPs of level k at a given phase. Alternative, albeit equivalent, formulations can be derived for the phase-shifting matrices of (15) if matrices $\mathbf{E}_{n_d \bmod M}(z)$ and $\mathbf{R}_{n_s \bmod M}(z)$ are respectively replaced based on (2) and (4)

$$\mathbf{F}_{m,i}^{l+1}(z) = \mathbf{E}_0(z) \left(z^{-1} \mathbf{P}_{n_d \bmod M}(z) \mathbf{P}_{M-n_s \bmod M}(z) \cdot \left[\mathbf{G}_{m,i}^l(z) \right]_0 + \sum_{q=1}^{M-1} z^{-2} \left[\mathbf{G}_{m,i}^l(z) \right]_q \right) \cdot \mathbf{P}_{n_d \bmod M}(z) \mathbf{P}_q(z) \mathbf{P}_{M-n_s \bmod M}(z) \mathbf{R}_0(z). \quad (17)$$

Several formulations may be obtained from (17) by replacing the products of the pseudocircular matrices based on (8) or (9), as appropriate.

TABLE II

COMPARISON BETWEEN THE PROPOSED DIRECT PHASE SHIFTING AND THE CONVENTIONAL MULTIRATE APPROACH (WHICH OPERATES AS SHOWN IN FIG. 1 AND PERFORMS M SHIFTS AT EACH NODE FOR THE CONSTRUCTION OF ALL THE PHASES OF THE TIDWP DECOMPOSITION). “FILTERS” IS THE NUMBER OF FILTER KERNELS (LOW-PASS AND HIGH-PASS) APPLIED TO THE INPUT FOR THE PRODUCTION OF THE RESULTS, WHILE “MEMORY” IS THE MAXIMUM NUMBER OF REQUIRED WAVELET COEFFICIENTS FOR THE PRODUCTION OF THE TIDWP DECOMPOSITION. THE LAST COLUMN SHOWS THE REDUCTION IN EXECUTION TIME OFFERED BY THE PROPOSED SUCCESSIVE PHASE-SHIFTING APPROACH VERSUS THE LIFTING-BASED IMPLEMENTATION OF THE CONVENTIONAL MULTIRATE APPROACH

Decomposition level k	Proposed method		Multirate method		Average reduction in execution time offered by the proposed method (%)
	Filters	Memory	Filters	Memory	
1	12288	8192	8192	12288	57.14
2	40960	8192	24576	24576	54.55
3	110592	8192	57344	57344	44.00
4	278528	8192	122880	122880	-33.00 (increase)

Finally, the multidimensional extension of the generalized case of Proposition 3 is straightforward, by using independent one-dimensional constructions along each direction. For example, for the case of a TIDWP transform of level k for a $C \times R$ image, first, all the row phases $(n_{\text{row}}, 0)$ are constructed, followed by the column phases $(n_{\text{row}}, n_{\text{col}})$, for each $0 \leq n_{\text{row}}, n_{\text{col}} \leq M^k - 1$.

III. IMPLEMENTATION TRADEOFFS OFFERED BY THE PROPOSED APPROACH

In general, the conventional multirate construction of the TIDWP transform starting from the input signal consists of the algorithm with the minimum computational complexity. However, there are two disadvantages for this approach.

- 1) Increasing memory resources are required for higher decomposition levels. For example, for any level k , $N \cdot (M^{k+1} - M)$, wavelet coefficients are produced in order to construct the TIDWP transform of an N -sample signal. This is disadvantageous since arithmetic operations are, by far, less energy and time consuming than on-chip and (especially) off-chip memory accesses in custom-hardware or programmable-processor realizations.
- 2) The calculation order does not match the bottom-up approach followed in best-basis algorithms [4], [8], since the fine-scale resolutions are required for the production of the coarse-scale ones. In addition, although many best-basis algorithms in the TIDWP domain may only utilize certain phase components depending on *a priori* knowledge in order to limit complexity (e.g., *a priori* knowledge of signal statistics), selective or localized phase construction is not facilitated by the conventional approach.

Previous research has shown that increasing the memory locality in the execution of such data-intensive algorithms is of paramount importance [22]. This indicates that, although the conventional multirate method for the TIDWP decomposition is computationally efficient, it can be overall impractical due to the large memory-access bottleneck. To this end, the proposed approach can provide viable alternatives.

For example, since most TIDWP-based applications can operate independently on each phase component of the decomposition (e.g., applications based on best-basis algorithms), the direct phase shifting requires a fixed amount of memory for the calculation and storage of each phase component of the TIDWP of every level k , equal to $2N$ coefficients. An example of the number of applied filter-kernels, the required memory resources and the execution times obtained by both methods for the popular case of $M = 2$ and $K = 1, \dots, 4$ is found in Table II. All compared algorithms were implemented in “C” and executed in an Intel Pentium IV processor with 32 Kb L1 (internal) data cache and 2 Mb L2 (external) cache. A 4096-sample signal was used and the 9/7 filter-pair was chosen for our experiments, implemented with floating-point accuracy (4 bytes per coefficient). The proposed approach performed successive phase shifting from phase $n_d - 1$ to n_d ($1 \leq n_d \leq$

$2^k - 1$). The zero-phase wavelet coefficients of each level k were generated with the lifting-based critically sampled discrete wavelet packet decomposition, whose execution time (and required computational and memory overhead) was included in the comparison.

Profiling of the execution of the proposed method verified that, although it generally requires more instruction-related operations in the case of lifting-based implementations, a significantly better utilization of the cache memory is achieved in comparison to the conventional multirate approach. As a result, the stall cycles in the CPU due to L1 (internal) data cache-related penalties are insignificant in the proposed approach in comparison to the conventional multirate method. We have obtained similar results for a variety of wavelet filter pairs, and it appears that the execution time reduction depends mostly on the number of decomposition levels.

In general, since each method is beneficial for a certain aspect (memory or computation), a combination of both approaches, i.e., phase-shifting combined with forward or inverse transforms can provide the optimum operation for a particular application. In addition, similar to our prior work [19], [20], filter symmetries can be utilized for the reduction of the arithmetic operations in the proposed approach, especially if multiple phase components can be kept in memory. These modifications may provide tradeoffs in computational resources versus memory requirements.

IV. CONCLUSION

A novel construction of an arbitrary-phase critically sampled discrete wavelet packet representation was presented. At any resolution level of an M -band discrete wavelet packet transform, the proposed method derives any desired phase component starting from any other phase of the critically sampled discrete wavelet packet representation of the same level. The proposed method is the most direct approach since it consists of the single-rate filtering of the input wavelet packet subbands with a set of phase-shifting matrices. This provides inherent advantages in the minimization of the intermediate memory required for the calculation, albeit with an increase in the required computations. Hence, depending on the utilization scenario, a hybrid algorithm combining direct phase shifting with multirate decomposition or reconstruction can provide the optimum realization for a particular problem.

APPENDIX I

Proof of Proposition 2: Initially, it is noted that, by the definition of l and n_s, n_d , for $k = 2$, we have $0 \leq l \leq 1$.

For the case of $l = 0$, we can follow the same logic as in Proposition 1 and establish that the proposition is true since, for every $0 \leq m \leq M - 1$, all packets $[\mathbf{w}_m^2(z)]_{n_s}$ and $[\mathbf{w}_m^2(z)]_{n_d}$ share the same “parent” subband at level one, which is $[\mathbf{S}_{m,0}^1(z)]_{\lfloor n_s/M \rfloor}$ (since $l = 0$, it follows that $\lfloor n_s/M \rfloor = \lfloor n_d/M \rfloor$). A pictorial illustration of this dependency is given in Fig. 1 for $M = 2$. Notice that, for this case, the

choice of the starting-phase WP index is $M^l \lfloor m/M^l \rfloor + i = m$, which ensures that the appropriate WP will be chosen by the phase shifting process of (10) depending on the value of m . Hence, the proposition is proven for this case.

For the remaining case of $l = 1$, where we have $M^l \lfloor m/M^l \rfloor + i = i$, we begin by constructing the WP $[\mathbf{w}_0^1(z)]_{n_s/M}$ as

$$[\mathbf{w}_0^1(z)]_{\lfloor n_s/M \rfloor} = \begin{bmatrix} \mathcal{D}^{-1} \mathbf{R}_{n_s \bmod M}(z) [\mathbf{w}_0^2(z)]_{n_s} \\ \vdots \\ \mathcal{D}^{-1} \mathbf{R}_{n_s \bmod M}(z) [\mathbf{w}_{M-1}^2(z)]_{n_s} \end{bmatrix}. \quad (18)$$

Subsequently, due to the fact that $l = 1$, it is guaranteed that $\lfloor n_s/M \rfloor \neq \lfloor n_d/M \rfloor$. Hence, we can apply a part of Proposition 1 to construct any subband $[S_{m,0}^1(z)]_{\lfloor n_d/M \rfloor}$

$$[S_{m,0}^1(z)]_{\lfloor n_d/M \rfloor} = [F_{m,0}^1(z) \ \cdots \ F_{m,M-1}^1(z)] [\mathbf{w}_0^1(z)]_{\lfloor n_s/M \rfloor}. \quad (19)$$

In order to reach $[w_m^2(z)]_{n_d}$, for any $0 \leq m \leq M-1$, we have to decompose subband $[S_{m,0}^1(z)]_{\lfloor n_d/M \rfloor}$ with the analysis polyphase matrix $\mathbf{E}_{n_d \bmod M}(z)$. This dependency is illustrated in the example of Fig. 1 for $M = 2$, where all even-numbered WPs of level two are produced by $A_0^1(z)$ (which is $S_{0,0}^1(z)$) and all odd-numbered WPs are produced by $D_0^1(z)$ (which is $S_{1,0}^1(z)$). After the decomposition of $[S_{m,0}^1(z)]_{\lfloor n_d/M \rfloor}$ of (19) with $\mathbf{E}_{n_d \bmod M}(z)$, the resulting expression can be expanded based on (18) and the first Noble identity [21]:

$$\begin{aligned} & [\mathbf{w}_m^2(z)]_{n_d} \\ &= \mathbf{E}_{n_d \bmod M}(z) \\ & \cdot \sum_{i=0}^{M-1} \left([F_{m,i}^1(z)]_0 \mathbf{I} + \sum_{q=1}^{M-1} z^{-1} [F_{m,i}^1(z)]_q \mathbf{P}_q(z) \right) \\ & \cdot \mathbf{R}_{n_s \bmod M}(z) [\mathbf{w}_i^2(z)]_{n_s}. \end{aligned} \quad (20)$$

It is straightforward to verify that (20) corresponds to (10) for $l = 1$. ■

APPENDIX II

Proof of Proposition 3: The proof is inductive. Initially, it is noted that the proposition holds for $E = 1, 2$ since it corresponds to Proposition 1 and Proposition 2, respectively. Subsequently, we assume that the proposition holds for level $E = k$. It is now proven that, given the WPs $[\mathbf{w}_0^{k+1}(z)]_{n_s}, \dots, [\mathbf{w}_{M^{k-1}}^{k+1}(z)]_{n_s}$, if (14) holds for $E = k$, it also holds for $E = k + 1$.

For level $k + 1$, by the definition of l , we have $0 \leq l \leq k$. Moreover, $0 \leq m \leq M^k - 1$. First, we construct all the WPs

$$[\mathbf{w}_{M^l \lfloor m/M^{l+1} \rfloor}^k(z)]_{\lfloor n_s/M \rfloor}, [\mathbf{w}_{M^l \lfloor m/M^{l+1} \rfloor + 1}^k(z)]_{\lfloor n_s/M \rfloor}, \dots, [\mathbf{w}_{M^l \lfloor m/M^{l+1} \rfloor + M^{l-1}}^k(z)]_{\lfloor n_s/M \rfloor}$$

as (21), shown at the bottom of the page.

For $l = 0$, we reach $[\mathbf{w}_m^{k+1}(z)]_{n_d}$ by a decomposition of subband $[S_{m \bmod M, \lfloor m/M \rfloor}^k(z)]_{\lfloor n_s/M \rfloor}$ derived in (21) with $\mathbf{E}_{n_d \bmod M}(z)$ since

we have $\lfloor n_s/M \rfloor = \lfloor n_d/M \rfloor$ for this case, i.e., both $[\mathbf{w}_m^{k+1}(z)]_{n_s}$ and $[\mathbf{w}_m^{k+1}(z)]_{n_d}$ packets have the same ‘‘parent’’ subband at decomposition level k . Hence, we derive (14) for the special case of $\mathbf{F}_{m,i}^1(z) \equiv \mathbf{F}^1(z)$, i.e., with the replacement of k by $k + 1$. This concludes the proof for this case.

For the remaining cases, for each $m = M \cdot x + j$, $0 \leq j \leq M - 1$, $x \in \mathbb{N}$, we can apply a part of (14) to construct subband $[S_{j, \lfloor m/M \rfloor}^k(z)]_{\lfloor n_d/M \rfloor}$ by the derived WPs of (21), since it is true by assumption. Also, due to the fact that $l > 0$, we have $\lfloor n_s/M \rfloor \neq \lfloor n_d/M \rfloor$, hence the proposition is applicable for our case:

$$\begin{aligned} & [S_{j, \lfloor m/M \rfloor}^k(z)]_{\lfloor n_d/M \rfloor} \\ &= \sum_{i=0}^{M^l-1} \left[G_{m, i \cdot M}^{l+1}(z) \ \cdots \ G_{m, i \cdot M + M - 1}^{l+1}(z) \right] \\ & \cdot [\mathbf{w}_{M^l \lfloor m/M^{l+1} \rfloor + i}^k(z)]_{\lfloor n_s/M \rfloor}. \end{aligned} \quad (22)$$

Notice that we chose to create subband $[S_{j, \lfloor m/M \rfloor}^k(z)]_{\lfloor n_d/M \rfloor}$ since it consists of the ‘‘parent’’ subband of the target WP $[\mathbf{w}_m^{k+1}(z)]_{n_d}$. A pictorial example is given in Fig. 1 for levels $k = 2, 3$ and $M = 2$. We can reach $[\mathbf{w}_m^{k+1}(z)]_{n_d}$ by decomposing $[S_{j, \lfloor m/M \rfloor}^k(z)]_{\lfloor n_d/M \rfloor}$ with $\mathbf{E}_{n_d \bmod M}(z)$ and expanding the resulting expression based on (21) and the first Noble identity [21]:

$$\begin{aligned} & [\mathbf{w}_m^{k+1}(z)]_{n_d} \\ &= \mathbf{E}_{n_d \bmod M}(z) \\ & \cdot \sum_{i=0}^{M^l-1} \sum_{v=0}^{M-1} \left([G_{m, M \cdot i + v}^{l+1}(z)]_0 \mathbf{I} \right. \\ & \quad \left. + \sum_{q=1}^{M-1} z^{-1} [G_{m, M \cdot i + v}^{l+1}(z)]_q \mathbf{P}_q(z) \right) \\ & \cdot \mathbf{R}_{n_s \bmod M}(z) [\mathbf{w}_{M^{l+1} \lfloor m/M^{l+1} \rfloor + M \cdot i + v}^{k+1}(z)]_{n_s}. \end{aligned} \quad (23)$$

The last equation can be simplified further if we set $i' = M \cdot i + v$, i.e., $v = i' \bmod M$ for $0 \leq v \leq M - 1$, as follows:

$$\begin{aligned} & [\mathbf{w}_m^{k+1}(z)]_{n_d} \\ &= \mathbf{E}_{n_d \bmod M}(z) \\ & \cdot \sum_{i'=0}^{M^{l+1}-1} \left([G_{m, i'}^{l+1}(z)]_0 \mathbf{I} \right. \\ & \quad \left. + \sum_{q=1}^{M-1} z^{-1} [G_{m, i'}^{l+1}(z)]_q \mathbf{P}_q(z) \right) \\ & \cdot \mathbf{R}_{n_s \bmod M}(z) [\mathbf{w}_{M^{l+1} \lfloor m/M^{l+1} \rfloor + i'}^{k+1}(z)]_{n_s}. \end{aligned} \quad (24)$$

It is straightforward to verify that (24) corresponds to (14) with $l' = l + 1$ and, therefore, $l \leq l' \leq k$. Moreover, $0 \leq l' \leq M^{l'} - 1$. As a result, (24) corresponds to (14) with k replaced by $k + 1$. This means that the proposition is true for the case of $E = k + 1$. Consequently, by induction, it is true for any level E , $E \geq 1$. ■

$$[\mathbf{w}_{M^l \lfloor m/M^{l+1} \rfloor + i}^k(z)]_{\lfloor n_s/M \rfloor} = \begin{bmatrix} \mathcal{D}^{-1} \mathbf{R}_{n_s \bmod M}(z) [\mathbf{w}_{M^{l+1} \lfloor m/M^{l+1} \rfloor + M i}^{k+1}(z)]_{n_s} \\ \vdots \\ \mathcal{D}^{-1} \mathbf{R}_{n_s \bmod M}(z) [\mathbf{w}_{M^{l+1} \lfloor m/M^{l+1} \rfloor + M i + M - 1}^{k+1}(z)]_{n_s} \end{bmatrix} \text{ with } 0 \leq i \leq M^l - 1. \quad (21)$$

REFERENCES

- [1] S. G. Mallat, *A Wavelet Tour of Signal Processing*. San Diego, CA: Academic, 1998.
- [2] R. R. Coifman and M. V. Wickerhauser, "Entropy-based algorithms for best-basis selection," *IEEE Trans. Inf. Theory*, vol. 38, no. 2, pp. 713–718, Mar. 1992.
- [3] K. Ramchandran, M. Vetterli, and C. Herley, "Wavelets, subband coding, and best bases," *Proc. IEEE*, vol. 84, pp. 541–560, 1996.
- [4] J. Liang and T. W. Parks, "A translation-invariant wavelet representation algorithm with applications," *IEEE Trans. Signal Process.*, vol. 44, no. 2, pp. 225–232, Feb. 1996.
- [5] J. -C. Pesquet, H. Krim, and H. Carfantan, "Time-invariant orthonormal wavelet representations," *IEEE Trans. Signal Process.*, vol. 44, no. 8, pp. 1964–1970, Aug. 1996.
- [6] S. D. Marco and J. Weiss, "Improved transient signal detection using a wavepacket-based detector with an extended translation-invariant wavelet transform," *IEEE Trans. Signal Process.*, vol. 45, no. 4, pp. 841–850, Apr. 1997.
- [7] R. R. Coifman and D. L. Donoho, "Translation invariant de-noising," in *Wavelets and Statistics: Lecture Notes in Statistics 103*, A. Antoniadis and G. Oppenheim, Eds. New York: Springer-Verlag, 1995, pp. 125–150.
- [8] N. Hess-Nielsen and M. V. Wickerhauser, "Wavelets and time-frequency analysis," *Proc. IEEE*, vol. 84, pp. 523–540, 1996.
- [9] A. F. Abdelnour and I. W. Selesnick, "Symmetric nearly shift invariant tight frame wavelets," *IEEE Trans. Signal Process.*, vol. 53, no. 1, pp. 231–239, Jan. 2005.
- [10] N. G. Kingsbury, "Complex wavelets for shift invariant analysis and filtering of signals," *J. Appl. Comput. Harmon. Anal.*, vol. 10, pp. 234–253, 2001.
- [11] M. Acharyya, R. K. De, and M. K. Kundu, "Extraction of features using M-band wavelet packet frame and their neuro-fuzzy evaluation for multitexture segmentation," *IEEE Trans. Pattern Anal. Mach. Intell.*, vol. 25, no. 12, pp. 1639–1644, Dec. 2003.
- [12] —, "Segmentation of remotely sensed images using wavelet features and their evaluation in soft computing framework," *IEEE Trans. Geosci. Remote Sens.*, vol. 41, no. 12, pp. 2900–2905, Dec. 2003.
- [13] F. Sinaga, E. Ambikairajah, and A. P. Bradley, "Over-sampling for accurate masking threshold calculation wavelet packet audio coders," in *IEEE Proc. Int. Conf. Communications Systems*, 2004, pp. 245–249.
- [14] B. S. Krongold, K. Ramchandran, and D. L. Jones, "Frequency-shift-invariant orthonormal wavelet packet representations," *IEEE Trans. Signal Process.*, vol. 47, no. 9, pp. 2579–2581, Sep. 1999.
- [15] I. Cohen, S. Raz, and D. Malah, "Shift invariant wavelet packet bases," in *Proc. IEEE Int. Conf. Acoustics, Speech, Signal Processing*, 1995, vol. 2, pp. 1081–1084.
- [16] A. T. Walden and A. C. Cristian, "The phase-corrected undecimated discrete wavelet packet transform and its application to interpreting the timing of events," *Proc. R. Soc. Lond. A, Math. Phys. Sci.*, vol. 454, pp. 2243–2266, 1998.
- [17] G. Van der Auwera, A. Munteanu, P. Schelkens, and J. Cornelis, "Bottom-up motion compensated prediction in the wavelet domain for spatially scalable video coding," *IEE Electron. Lett.*, vol. 38, pp. 1251–1253, 2002.
- [18] X. Li, "New results on phase shifting in the wavelet space," *IEEE Signal Process. Lett.*, vol. 10, no. 7, pp. 193–195, Jul. 2003.
- [19] Y. Andreopoulos, A. Munteanu, G. Van der Auwera, J. Cornelis, and P. Schelkens, "Complete-to-overcomplete discrete wavelet transforms: Theory and application," *IEEE Trans. Signal Process.*, vol. 53, no. 4, pp. 1398–1412, Apr. 2005.
- [20] —, "Single-rate calculation of overcomplete discrete wavelet transforms for scalable coding applications," *Signal Process.*, vol. 85, pp. 1103–1124, 2005.
- [21] P. P. Vaidyanathan, *Multirate Systems and Filter Banks*, 1st ed. Taipei, Taiwan, R.O.C.: Pearson Education, Inc., 1993.
- [22] N. D. Zervas, G. P. Anagnostopoulos, V. Spiliotopoulos, Y. Andreopoulos, and C. E. Goutis, "Evaluation of design alternatives for the 2-D discrete wavelet transform," *IEEE Trans. Circuits Syst. Video Technol.*, vol. 11, no. 12, pp. 1246–1262, Dec. 2001.

Myriad-Type Polynomial Filtering

Tuncer C. Aysal, *Student Member, IEEE*, and
Kenneth E. Barner, *Senior Member, IEEE*

Abstract—Linear combinations of polynomial terms yield poor performance in environments characterized by heavy-tailed distributions. Weighted myriad (WMy) filters, however, are well known for their outlier suppression and detail preservation properties. It is shown here that the WMy methodology is naturally extended to the polynomial sample case, yielding filter structures that exploit the higher order statistics of the observed samples while simultaneously being robust to outliers for heavy-tailed distributions environments. Moreover, the introduced power weighted myriad (PWMy) filter class is well motivated by analysis of cross- and square-term statistics of heavy-tailed distributions. The effectiveness of the proposed filter is evaluated through simulations.

Index Terms— α -stable distributions, impulsive processes, myriad filters, polynomial filtering, Volterra series.

I. INTRODUCTION

Nonlinear systems are at the heart of many contemporary signal processing problems. A nonlinear input–output characterization that is particularly amenable to analysis and synthesis is the discrete Volterra series representation [1]. Nonlinear systems are, in many cases, effectively represented by truncated Volterra series, which results in simpler realization that requires limited knowledge of higher order statistics [2]. Although the order of polynomial terms in the Volterra series extends to infinity, many practical problems are effectively addressed with second-order Volterra filters, which are restricted to include only linear and second-order quadratic components [2]–[5].

The polynomial nature of the Volterra filter leads to poor performance in environments characterized by impulsive distributions. Clearly, quadratic terms residing in the second-order kernels of the filter amplify the damaging effects of present outliers. To address the robustness issue, the polynomial weighted median (PWM) filter structure was recently proposed [6]. The PWM is robust to outliers while still exploiting the higher order statistics of observed samples. The PWM filter structure is, however, based on the assumption that the observed samples obey Laplacian statistics, yielding a filter output formulation given by the weighted sum of subweighted median (WM) filter outputs. An important shortcoming of the WM-type filters is that their output is always constrained, by definition, to one of the samples in the window. Although, this *selection* characteristic is desirable in, for example image processing applications [7], it results in efficiency losses for many other applications [8]. It can be argued that the inefficiency of median-based methods in practical problems arises from their unsuitability for processing noise processes that are found in real applications. While most noise processes that appear in practice obey probability density functions (PDFs) that are *bell-shaped*, the Laplacian model, for which the median is optimal in the maximum-likelihood (ML) sense, has a *peaky* density that makes it, in general, rather artificial [7].

In this correspondence, the class of polynomial weighted myriad (PWMy) filters is proposed as a polynomial filtering framework with

Manuscript received August 30, 2005; revised March 31, 2006. The associate editor coordinating the review of this manuscript and approving it for publication was Prof. Tulay Adali.

The authors are with the Department of Electrical and Computer Engineering, University of Delaware, Newark, DE 19716 USA (e-mail: aysal@mail.eecis.udel.edu; barner@ece.udel.edu).

Digital Object Identifier 10.1109/TSP.2006.885758